

# MORPHOLOGICAL CHANGES OF HUMAN MESENCHYMAL STEM CELLS UNDER 3D CLINOSTAT CULTURE

HO NGUYEN QUYNH CHI<sup>1,2</sup> AND HOANG NGHIA SON<sup>1,2,\*</sup>

<sup>1</sup>Animal Biotechnology Department, Institute of Tropical Biology, Vietnam Academy of Science and Technology, Ho Chi Minh City, 700000, Vietnam

<sup>2</sup>Biotechnology Department, Graduate University of Science and Technology, Vietnam Academy of Science and Technology, Ha Noi, 100000, Vietnam

(Received 6 May, 2020; accepted 3 June, 2020)

**Key words :** Cytoskeleton, Mesenchymal stem cells, Microgravity, Morphology.

**Abstract** – This study aimed to estimate morphological changes of human mesenchymal stem cells (hMSCs) under 3D clinostat culture which generated simulated microgravity (SMG) condition. hMSCs were induced simulated microgravity ( $<10^{-3}$  G) for 3 days, while control group was conducted in the normal G condition (1G). The results showed that the cellular area of hMSCs from SMG group was higher than control group ( $14083.34 \pm 1069.38 \mu\text{m}^2$  vs.  $11368.67 \pm 535.27 \mu\text{m}^2$ , respectively). The FSC value of hMSCs from SMG group was higher than control group ( $10803988.58 \pm 20960.12$  vs.  $9829898.02 \pm 206370.30$ , respectively). Thus, SMG condition induced the increase in the size of hMSCs. Microtubule staining analysis demonstrated that the intensity of the microtubule of hMSCs from control group was higher than SMG group ( $3980694.27 \pm 842699.73$  vs.  $2860286.60 \pm 338612.60$ , respectively). Moreover, the intensity of the microfilament of hMSCs from control group was higher than SMG group ( $4276497.43 \pm 1190673.58$  vs.  $3364019.71 \pm 688901.20$ , respectively). In addition, SMG condition moderated hMSC nuclear morphology, in which the transformation of round-shape to oval-shape was observed in hMSCs induced by SMG. These results revealed that SMG condition modified the cytoskeleton distribution in hMSCs, which leads to the morphological changes.

## INTRODUCTION

Exposure to the microgravity environment has been shown to adversely affect organisms. Significant side effects of long-term weightlessness include muscle atrophy and skeletal insufficiency (Demontis *et al.*, 2017), changing red blood cell production (Udden *et al.*, 1995), and changing in the immune system (Crucian *et al.*, 2018). The weightlessness induces the reduction of body mass, telomere elongation, genome instability, metabolic changes (Garrett-Bakelman *et al.*, 2019). Studies on evaluating the effect of microgravity on organisms and cells have been carried out for a long time. However, the implementation of these experiments faces many difficulties due to the flight opportunities are very scarce and the costs of hardware development are high (Ulbrich *et al.*, 2014). Thus, the microgravity simulators have been developed and applied to estimate changes in structure, function, proliferation of mammalian cells. Clinostat is one of the first models which was invented at the end of the 19<sup>th</sup>

century (von Sachs, 1879). This was rotational devices and was mostly used to estimate the effect of simulated microgravity on plants. This model was improved into a fast-rotating clinostat which was applied for cell culture studies (Briegleb, 1967). Up to present, 3D clinostat and random positioning machine are the most common system using for animal cell studies (Hoson *et al.*, 1997; van Loon, 2007; Borst and van Loon, 2009). In this study, we applied 3D clinostat to evaluate the effects of SMG condition on morphological change of hMSCs. The morphology of hMSCs was assessed by cytoplasm and nuclear expansion, cell area, cell diameter, especially the intensity of microtubule and microfilament.

## MATERIALS AND METHODS

### Cell culture

hMSCs were cultured in 96-well plates and T-25 flask with DMEM F-12 (Capricorn Scientific,

Germany) supplemented with 15% FBS (Capricorn Scientific, Germany) and 1% Pen/Strep (Gibco, United States). hMSCs were induced SMG condition ( $<10^{-3}$  G) by 3D clinostat (MiGra-ITB, Vietnam Academy of Science and Technology) for 3 days at 37°C, 5 % CO<sub>2</sub>. The hMSCs of control group were treated at 1G in the same CO<sub>2</sub> incubator.

### Flow cytometry analysis

To estimate the cellular diameter, hMSCs were used for flow cytometry analysis. hMSCs were washed cold PBS and resuspended in 1X Binding Buffer at a concentration of  $1 \times 10^6$  cells/mL. 100  $\mu$ L of the solution ( $1 \times 10^5$  cells) was transferred to a 5 mL tube. 5  $\mu$ L PI was added to the tube and incubated for 15 min at RT (25°C) in the dark. 400  $\mu$ L of 1X Binding Buffer was added to each tube. The flow cytometry was performed within 1 hr.

### Microtubule staining

To evaluate microtubule intensity, hMSCs were cultured in 96-well plates and microtubule was labeled with 2  $\mu$ L SiR-tubulin (Cytoskeleton, Inc., United States). hMSCs were induced with SMG condition for 3 days. The microtubule of hMSCs was observed and assessed under Cytell microscope (GE Healthcare, United States).

### Microfilament staining

To evaluate microfilament intensity, hMSCs were cultured in 96-well plates and were treated with SMG condition in 72 hours. hMSCs were fixed by 4% paraformaldehyde (Nacalai, Japan) and permeabilized with 0.1% Triton X-100 (Merck, Germany). Microfilament of hMSCs was stained with Phalloidin Cruz Fluor™ 488 Conjugate (Santa Cruz Biotechnology, United States). Hoechst 33342 (Sigma-Aldrich, United States) was applied for nuclear staining of hMSCs. The stained hMSCs were observed and evaluated under Cytell microscope (GE Healthcare, United States).

### Area measurement

Cell area, morphology and intensity of microtubule and microfilament of hMSCs was evaluated by ImageJ software (National Institutes of Health, Bethesda, MD). Images were converted grayscale (type 8 bit) then subjected to the threshold function using the same threshold for all images to remove background noise and auto-fluorescence (Son *et al.*, 2019), then the cell areas and intensity of microtubule and microfilament were measured.

### Statistical analysis

The data were analyzed by one-way analysis of variance (ANOVA).  $P < 0.05$  was considered statistically significant.

## RESULTS

The present study applied the 3D clinostat to induce SMG on hMSCs. The cellular morphology of hMSCs was demonstrated in Figure 1A and 1B. hMSCs from SMG exposed the higher cytoplasmic expansion, comparing to hMSCs from control group. hMSCs from both groups exhibited the large, flattened, and spindle-shaped morphology. hMSCs showed normal proliferation. The apoptotic properties of cytoplasm were not observed in hMSCs from both control group and SMG group. The cellular area of hMSCs from SMG group was  $14083.34 \pm 1069.38 \mu\text{m}^2$  which was higher than hMSCs from control group ( $11368.67 \pm 535.27 \mu\text{m}^2$ ) ( $P = 0.022$ ) (Figure

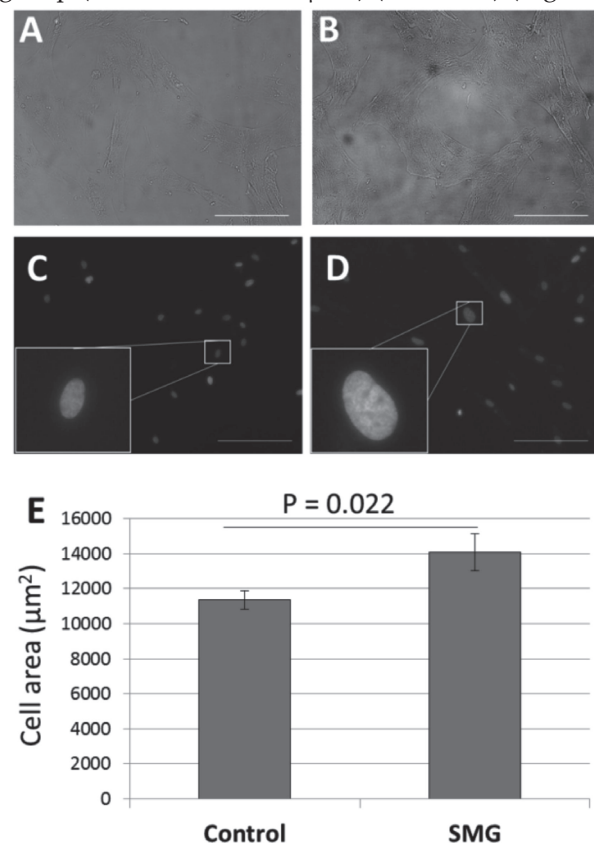


**Fig. 1.** Cellular and nuclear morphology of hMSCs. A, B: Cellular morphology of hMSCs from control group and SMG group. C, D: Nuclear morphology of hMSCs from control group and SMG group. E: Cell area was generated by Image J. Scale bar: 223.64  $\mu\text{m}$ .

1E). This result supported the cytoplasmic change of hMSCs under SMG condition. Moreover, hMSCs from control group showed the normal morphology of nuclear (Figure 1C), while morphological changes of nuclear were observed in hMSCs from SMG group. hMSC nuclear under SMG condition was expanded and has not exhibited in round-shaped morphology (Figure 1D).

The morphological changes of hMSCs under SMG condition was also assessed by flow cytometry analysis. As seen in Figure 2A and 2B, the FSC value of hMSC from SMG group was increased, demonstrating by the higher distribution in flow cytometry chart. The FSC value of hMSCs from SMG group was  $10803988.58 \pm 20960.12$  which was higher than hMSCs from control group ( $9829898.02 \pm 206370.30$ ) ( $P = 0.008$ ) (Figure 2C). This result indicated that SMG condition induced an increase of cellular diameter in hMSCs.

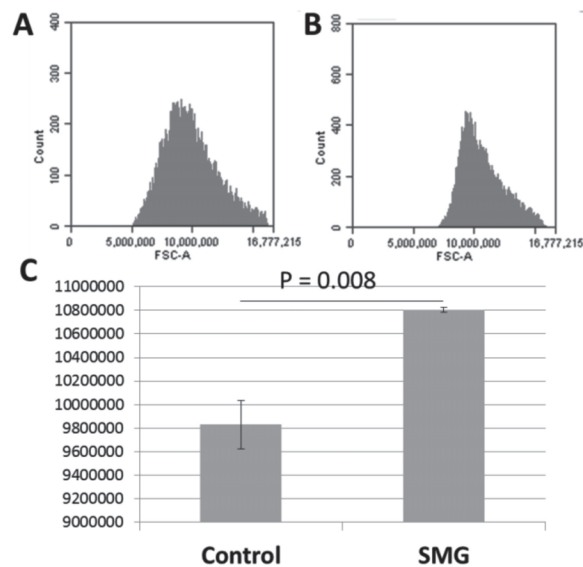


**Fig. 2.** Cellular diameter was performed by flow cytometry. A, B: FSC chart of hMSCs from control group and SMG group. C. Comparison of FSC value of hMSCs from control group and SMG group.

In the present investigation, we also estimated the changes of microtubule and microfilament in the cytoplasm of hMSCs. hMSCs from control group showed a higher density of microtubule in the cytoplasm, compared to hMSCs from SMG group (Figure 3A). The lower distribution was observed in hMSCs under SMG condition (Figure 3B). The intensity of the microtubule of hMSCs from control group was  $3980694.27 \pm 842699.73$  which was higher

than hMSCs from SMG group ( $2860286.60 \pm 338612.60$ ) (Figure 3C). This result showed SMG condition induced the diminished expression of microtubule in hMSCs.

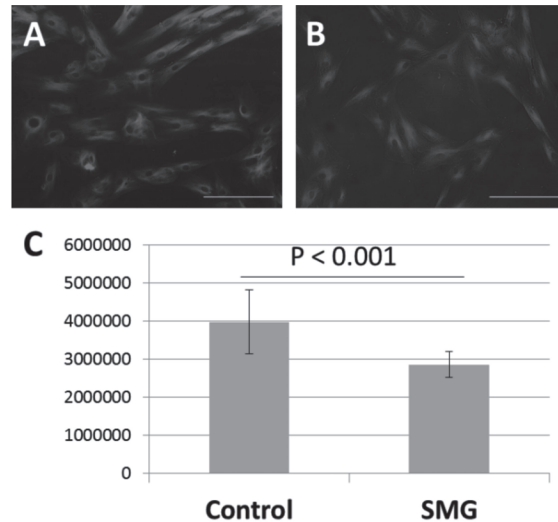


**Fig. 3.** Microtubule staining with Sir-Tubulin in hMSCs. A, B: The expression of microtubule (red color) of hMSCs from control group and SMG group. Intensity comparison of microtubule in hMSCs from control group and SMG group. Scale bar: 223.64  $\mu$ m

One of the important components of the cytoskeleton is microfilament which distributes to the formation of cell shape. Figure 4A showed a higher intensity of microfilament in hMSCs from control group, comparing to the hMSCs under SMG condition (Figure 4B). The intensity of the microfilament of hMSCs from control group was  $4276497.43 \pm 1190673.58$  which was higher than hMSCs from SMG group ( $3364019.71 \pm 688901.20$ ) (Figure 4C). This result showed SMG condition induced the diminished expression of microtubule in hMSCs.

## DISCUSSION

The present work demonstrated that SMG condition induced the morphological changes of hMSCs for 3 days culture. Previous studies have been demonstrated that SMG conditions can generate the morphological changes of mammalian cells by different mechanisms. SMG condition induced the changes in structural morphology such as cell shape and membrane roughness of human erythrocytes (Dinarelli *et al.*, 2018). Human primary osteoblasts exposed a morphological shift from flat-shape to

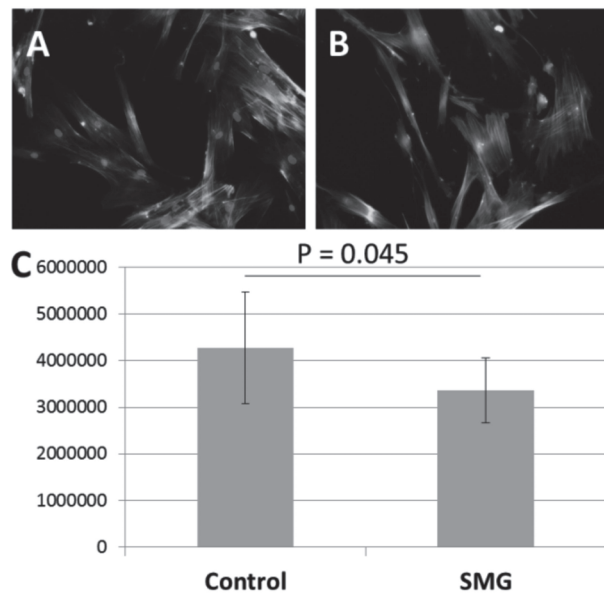


**Fig. 4.** Microfilament staining with Phalloidin in hMSCs. A, B: The expression of microfilament (green color) of hMSCs from control group and SMG group. Intensity comparison of microfilament in hMSCs from control group and SMG group. Scale bar: 223.64  $\mu\text{m}$ .

spindle-shape, in which the majority of cell population under SMG condition exhibits the spindle-shaped cell morphology (Gioia *et al.*, 2018). SMG condition also induces the changing of actin cytoskeleton and variation in the presence in human A431 cells (Moes *et al.*, 2011). Another study reported that SMG condition generated dramatic changes in the size and shape of the cells and their surface specializations (Kapitonova *et al.*, 2013). SMG condition induced by parabolic flight can modify the morphology in breast cancer cells, such as tubulin with holes, accumulations in the tubulin network, and the appearance of filopodia- and lamellipodia-like structures in the F-actin cytoskeleton shortly after the beginning of the microgravity (Nassef *et al.*, 2019). In this study, we found that the SMG condition induced the changes of hMSC morphology, especially cytoplasm and cytoskeleton. The increase of cellular diameter resulted in the enlargement of the cytoplasm of hMSCs under SMG condition. Moreover, the cytoskeleton plays an essential role in organizing cell structures, supporting to shape changing (Fletcher and Mullins, 2010). The modifications of cytoskeleton or cytoskeletal protein synthesis associate with changes in cellular shape and organization. This investigation demonstrated that

the intensity of microtubule and microfilament was reduced in hMSCs induced by SMG condition, leading to the change of distribution and the reorganization of the cytoskeleton.

## CONCLUSION

The present study demonstrated that simulated microgravity could produce morphological changes in hMSCs. The redistribution and reorganization of cytoskeleton were given the rise in hMSCs under simulated microgravity condition.

## ACKNOWLEDGMENTS

This work was supported by grant VT-CB.15/18-20 of Space Science and Technology Program from Vietnam Academy of Science and Technology.

## REFERENCES

- Borst, A.G. and van Loon, J. 2009. Technology and Developments for the Random Positioning Machine, RPM. *Microgravity Sci. Technol.* 21 : 287-292.
- Briegleb, W. 1967. Ein Modell zur Schwerelosigkeitssimulation an Mikroorganismen. *Naturwissenschaften.* 54 : 167.
- Crucian, B.E., Choukèr, A., Simpson, R.J., Mehta, S., Marshall, G., Smith, S.M., Zwart, S.R., Heer, M., Ponomarev, S., Whitmire, A., Fripiat, J.P., Douglas, G.L., Lorenzi, H., Buchheim, J.I., Makedonas, G., Ginsburg, G.S., Ott, C.M., Pierson, D.L., Krieger, S.S., Baecker, N. and Sams, C. 2018. Immune System Dysregulation During Spaceflight: Potential Countermeasures for Deep Space Exploration Missions. *Front Immunol.* 9 : 1437.
- Demontis, G.C., Germani, M.M., Caiani, E.G., Barravecchia, I., Passino, C. and Angeloni, D. 2017. Human Pathophysiological Adaptations to the Space Environment. *Front Physiol.* 8 : 547.
- Dinarelli, S., Longo, G., Dietler, G., Francioso, A., Mosca, L., Pannitteri, G., Boumis, G., Bellelli, A. and Girasole, M. 2018. Erythrocyte's aging in microgravity highlights how environmental stimuli shape metabolism and morphology. *Sci. Rep.* 8 (1) : 5277.
- Fletcher, D.A. and Mullins, R.D. 2010. Cell mechanics and the cytoskeleton. *Nature.* 463 : 485-492.
- Garrett-Bakelman, F.E., Darshi, M., Green, S.J., Gur, R.C., Lin, L., Macias, B.R., Mc Kenna, M.J., Meydan, C., Mishra, T., Nasrini, J., Piening, B.D., Rizzardi, L.F., Sharma, K., Siamwala, J.H., Taylor, L., Vitaterna, M.H., Afkarian, M., Afshinnekoo, E., Ahadi, S., Ambati, A., Arya, M., Bezdán, D., Callahan, C.M., Chen, S., Choi, A.M.K., Chlipala, G.E., Contrepois, K., Covington, M., Crucian, B.E., De Vivo, I., Dinges, D.F., Ebert, D.J., Feinberg, J.I., Gandara, J.A., George,

- K.A., Goutsias, J., Grills, G.S., Hargens, A.R., Heer, M., Hillary, R.P., Hoofnagle, A.N., Hook, V.Y.H., Jenkinson, G., Jiang, P., Keshavarzian, A., Laurie, S.S., Lee-McMullen, B., Lumpkins, S.B., MacKay, M., Maienschein-Cline, M.G., Melnick, A.M., Moore, T.M., Nakahira, K., Patel, H.H., Pietrzyk, R., Rao, V., Saito, R., Salins, D.N., Schilling, J.M., Sears, D.D., Sheridan, C.K., Stenger, M.B., Tryggvadottir, R., Urban, A.E., Vaisar, T., Van Espen, B., Zhang, J., Ziegler, M.G., Zwart, S.R., Charles, J.B., Kundrot, C.E., Scott, G.B.I., Bailey, S.M., Basner, M., Feinberg, A.P., Lee, S.M.C., Mason, C.E., Mignot, E., Rana, B.K., Smith, S.M., Snyder, M.P. and Turek, F.W. 2019. The NASA Twins Study: A multidimensional analysis of a year-long human spaceflight. *Science*. 364 (6436) : eaau8650.
- Gioia, M., Michaletti, A., Scimeca, M., Marini, M., Tarantino, U., Zolla, L. and Coletta, M. 2018. Simulated microgravity induces a cellular regression of the mature phenotype in human primary osteoblasts. *Cell Death Discov*. 4 : 59.
- Hoson, T., Kamisaka, S., Masuda, Y., Yamashita, M. and Buchen, B. 1997. Evaluation of the Three-Dimensional Clinostat as a Simulator of Weightlessness. *Planta*. 203 : S187-S197.
- Kapitonova, M.Y., Salim, N., Othman, S., Muhd Kamauzaman, T.M., Ali, A.M., Nawawi, H.M. and Froemming, G.R. 2013. Alteration of cell cytoskeleton and functions of cell recovery of normal human osteoblast cells caused by factors associated with real space flight. *Malays J Pathol*. 35 (2) : 153-163.
- Moes, M.J.A., Gielen, J.C., Bleichrodt, R., van Loon, J.J.W.A., Christianen, P.C.M. and Boonstra, J. 2011. Simulation of Microgravity by Magnetic Levitation and Random Positioning: Effect on Human A431 Cell Morphology. *Microgravity Sci. Technol*. 23 : 249-261.
- Nassef, M.Z., Kopp, S., Wehland, M., Melnik, D., Sahana, J., Krüger, M., Corydon, T.J., Oltmann, H., Schmitz, B., Schütte, A., Bauer, T.J., Infanger, M. and Grimm, D. 2019. Real Microgravity Influences the Cytoskeleton and Focal Adhesions in Human Breast Cancer Cells. *Int. J. Mol. Sci*. 20 : 3156.
- Son, H.N., Chi, H.N.Q., Chung, D.C. and Long, L.T. 2019. Morphological changes during replicative senescence in bovine ovarian granulosa cells. *Cell Cycle*. 18 (13) : 1490-1497.
- Udden, M.M., Driscoll, T.B., Pickett, M.H., Leach-Huntoon, C.S. and Alfrey, C.P. 1995. Decreased production of red blood cells in human subjects exposed to microgravity. *J. Lab. Clin. Med*. 125 (4) : 442-449.
- Ulbrich, C., Wehland, M., Pietsch, J., Aleshcheva, G., Wise, P., van Loon, J., Magnusson, N., Infanger, M., Grosse, J., Eilles, C., Sundaresan, A. and Grimm, D. 2014. The impact of simulated and real microgravity on bone cells and mesenchymal stem cells. *Biomed Res Int*. 2014: 928507.
- Van Loon, J.J.W.A. 2007. Some History and Use of the Random Positioning Machine, RPM, in Gravity Related Research. *Adv. Space Res*. 39 : 1161-1165.
- Von Sachs, J. 1879. Über Ausschliessung der geotropischen und heliotropischen Krümmungen während des Wachstums. *Würzburger Arbeiten*. 2 : 209-225.
- 
-